Electrophoresis simulated with the cage model for reptation

A. van Heukelum and H. R. W. Beljaars
Institute for Theoretical Physics, Utrecht University, Princetonplein 5, 3584 CC Utrecht, The Netherlands

(Received 25 February 2000; accepted 6 June 2000)

The cage model for polymer reptation is extended to simulate gel electrophoresis. With increasing electric field strength E, the drift velocity v of a long polymer with length L shows three different regimes: (a) the linear regime where $v \sim E/L$; (b) the quadratic regime where $v \sim E^2$, independent of the length of the polymer; and (c) a regime where the velocity decreases exponentionally with E. The transition between regimes (a) and (b) occurs for field strengths $E \sim L^{-1}$. The transition between regimes (b) and (c) occurs for some value E_h, for which $L^{-1} \ll E_h \ll 1$. The behavior in the first two regimes is in agreement with earlier reports on simulations of the Duke–Rubinstein model, and with experimental work on DNA polymers in agarose gel. The third regime is not reported for the Duke–Rubinstein model, probably because in this model, stored length cannot compile into hernias. © *2000 American Institute of Physics.* [S0021-9606(00)51633-X]

I. INTRODUCTION

Gel electrophoresis is a widely used tool to separate mixtures of DNA molecules by length. The DNA is confined to an agarose gel, and an electric field is applied. Since DNA is negatively charged, it moves towards the positive electrode as a result of this electric field. As the drift velocity depends on the length, DNA fragments with different lengths end up in different bands, and can therefore easily be separated.

Since DNA fragments are usually much longer than the typical spacing between the gel strands, they are unable to move sideways. De Gennes[1] described the motion of a polymer in such an environment, and termed it *reptation*: the polymers move by diffusion of ''defects'' along the chain of monomers. Each defect contracts the polymer by a certain amount of length, called its *stored length*. When a defect passes a monomer, the monomer is moved by this distance. Figure 1 shows an example where a defect travels through a polymer of three monomers.

Sideways movement is also largely prohibited in a dense polymer solution or a polymer melt. Therefore the main means of movement is believed to be reptation-like. Indeed, Perkins *et al.*,[2] show that a polymer in a melt is confined by a ''tube,'' by dragging a marked DNA strand through a dense solution of DNA strands.

Two models are widely used to simulate reptation: the repton model, introduced by Rubinstein,[3] and the cage model, introduced by Evans and Edwards.[4] In both models, monomers reside on sites of a simple cubic lattice (or in two dimensions a square lattice), and are connected by bonds; the dynamics consist of single-monomer moves.

In the repton model, stored length consists of zero-length bonds. For this model, it was proposed by Rubinstein,[3] and later proven by Prähofer and Spohn,[5] that the diffusion constant D of the polymer in the limit of long polymer length L obeys the scaling $L^2 D = 1/3$. For finite lengths, the diffusion constant is known numerically exact up to length 20 and from Monte Carlo simulations up to length 250.[6] The repton model has been adapted for the study of electrophoresis by Duke.[7] This Duke–Rubinstein model has been studied numerically for lengths up to 400.[8] Simulations of this model are easy because it can, without loss of generality, be reduced to a one-dimensional model.

In the cage model, stored length consists of a pair of antiparallel nearest-neighbor bonds, called *kinks*. The polymer diffusion constant in this model has been determined numerically exact for small polymer lengths,[9] and with Monte Carlo simulations for polymers up to length 200.[10–12] As in the repton model, the polymer diffusion constant scales as $D \sim L^{-2}$. In this work, we extend the cage model to simulate a charged polymer in an electric field. For this model, we find an exponential decrease of the polymer drift velocity, above some value E_h, $L^{-1} \ll E_h \ll 1$. This regime has not been found with the Duke–Rubinstein model, probably because of shortcomings of the Duke–Rubinstein model, as we will discuss in Sec. IV.

In Sec. II we describe the cage model and present how the model can be extended to simulate reptation in a nonzero electric field. In Sec. II B we discuss scaling arguments for the drift velocity. We present in Sec. III some technical details about how efficient simulations can be achieved with multispin coding. The simulation results are presented in Sec. IV which includes discussions about the polymer shapes, the distribution of stored length along the polymer, and comparison to previous reports.

II. CAGE MODEL

The cage model describes a polymer of L monomers, located on the sites of an infinite cubic lattice. The monomers are connected by $L-1$ bonds with a length of one lattice spacing. A single step of the Monte Carlo simulation consists of selecting randomly a monomer and, if it is free to move, moving it to a randomly selected location (possibly the current location).

The monomers at both ends of the polymer are always free to move, but monomers in the interior of the polymer

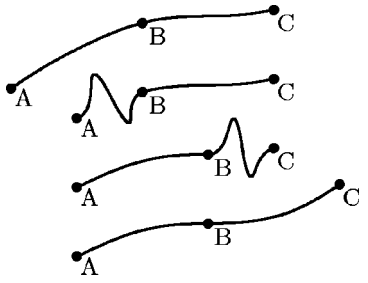

FIG. 1. Movement of a defect along the chain. When a defect moves along the chain, it displaces monomers which it passes by a distance equal to the stored length.

are only free to move when the two neighbors along the chain are located on the same adjacent lattice site. Other movements might result in an acceptable polymer configuration, but are ruled out because they would allow the polymer to move sideways, which is not reptation. One possible interior move is shown in Fig. 2. Every possible move occurs statistically with unit rate, setting the time scale. A single elementary move thus corresponds to a time increment of $\Delta t=(2dL)^{-1}$, where d is the dimensionality of the lattice; in our case, $d=3$.

A. Electric field

In solution, DNA becomes negatively charged with a fixed charge per unit length. We incorporate this into the cage model by assigning a charge q per monomer. The polymer is located in a homogeneous electric field $\vec{E}$, that acts on these charged monomers.

For two monomer positions $\vec{r}_1$ and $\vec{r}_2$, separated by a displacement $\vec{r}_{12}=\vec{r}_2-\vec{r}_1$, the difference in potential energy is given by $U=q\vec{E}\cdot\vec{r}_{12}$. The ratio of the corresponding Boltzmann probabilities is

$$P_1/P_2=e^{U/k_BT}=e^{qEr/k_BT}, \tag{1}$$

where $E=|\vec{E}|$ is the field strength, and $r=\vec{E}\cdot\vec{r}_{12}/|\vec{E}|$ is the displacement parallel to the field.

In a Monte Carlo simulation, this ratio determines at which rates the monomers are to be moved along the field or against it. We choose the direction of the electric field along one of the body diagonals of the unit cubes, because then the x, y, and z directions are equivalent, and within one elementary move, the displacement r takes only the two values $\pm 2/\sqrt{d}$ times the lattice spacing. For convenience, the units are chosen in such a way that $qr/k_BT=\pm 1$.

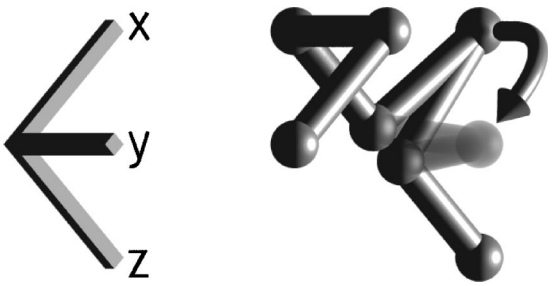

FIG. 2. One elementary move of a monomer: a ''kink'' (pair of antiparallel neighboring bonds) is replaced by another kink.

Each monomer moves with a rate $R^+=\exp(E)$ for moves which lower the energy and $R^-=\exp(-E)$ for moves which raise the energy. This is accomplished by randomly selecting a monomer, and, if it is free to move, choosing one of the possible $2d$ positions with certain probabilities. One-half of the possible positions have a lower energy; these are chosen with a probability P^+. The other positions have a higher energy and are chosen with a probability P^-. The probabilities P^+ and P^- are given by

$$P^+=\frac{1}{d}\frac{e^E}{e^E+e^{-E}}, \quad P^-=\frac{1}{d}\frac{e^{-E}}{e^E+e^{-E}}. \tag{2}$$

The time increment corresponding to one elementary Monte Carlo move is thus equal to

$$\Delta t=\frac{1}{dL}\frac{1}{e^E+e^{-E}}; \tag{3}$$

this reduces to $\Delta t=(2dL)^{-1}$ for $E\to 0$.

Contrary to the repton model, the cage model allows for the creation of so-called hernias. A *hernia* is a buildup of stored length that protrudes from the confining tube of the polymer. We will show that those hernias become important when the polymer is subjected to an electric field E_h, $L^{-1}\ll E_h\ll 1$. The difference between the drift velocities computed with the repton model and the cage model in these high electric fields is attributed to polymer configurations with hernias.

B. Scaling arguments for the drift velocity

The velocity of a polymer in a small electric field behaves according to the Nernst–Einstein relation, $v=FD$, where $F=qLE$ is the force. The diffusion constant can thus be calculated from the drift velocity by $D=v/qLE$ in the limit $E\to 0$. De Gennes[1] found the diffusion constant to be proportional to $D\sim L^{-2}$. This means the drift velocity is $v\sim qE/L$.

For slightly larger electric fields the Nernst–Einstein relation breaks down. Barkema, Marko, and Widom[8] give an intuitive explanation of the dependence of the drift velocity on the electric field strength. The argument goes as follows.

Monte Carlo chains, like continuous chains, transmit tension by an entropic process. A random polymer will have an end-to-end length around $h=\sqrt{L}$. When an electric field is applied, the polymer is stretched in the direction of the electric field. A stretched polymer configuration is entropically less favorable than a compact form: the result is an elastic force that contracts the polymer. When the electric field exceeds a certain level, the polymer as a whole no longer resembles a random walk: $h>\sqrt{L}$. One may cut the polymer into n_b pieces (*blobs*) of length $L_b=L/n_b$, that each still look like a random walk; the average end-to-end distance of the blobs is equal to $\langle h_b\rangle=\sqrt{L_b}$. The elastic force is proportional to the size of the blob and inversely proportional to the length of the part of the polymer that forms the

TABLE I. Encoding of a bond in three bits, where $x^{(i)}$ is the ith bit of x and so on. Note that the encoding of the negative bonds is the binary complement of the positive bonds.

	Bond direction					
Integer	**+x**	**+y**	**+z**	**−x**	**−y**	**−z**
$x^{(i)}$	1	0	0	0	1	1
$y^{(i)}$	0	1	0	1	0	1
$z^{(i)}$	0	0	1	1	1	0

blob: $F_{\text{elastic}} \sim h_b / L_b$. The electric force on a blob is proportional to the size of the blob as well as the electric field: $F_{\text{electric}} \sim h_b E$. These two forces have to be in balance which implies that the blob size is $L_b \sim E^{-1}$. The Nernst–Einstein relation now applies to the blobs, so $v = F_b D_b = q L_b E D_b$. Again, if the blob size is large enough, $D_b \sim L_b^{-2}$ which makes the speed of the polymer quadratic in the electric field: $v \sim qE/L_b \sim qE^2$. This effect has already been observed in the Duke–Rubinstein model by Barkema, Marko, and Widom.[8]

III. IMPLEMENTATION

As described in Sec. II the monomers are connected by bonds, where each bond has one of $2d$ possible orientations. One way of describing the polymer configuration is by specifying the location of the first monomer and the orientation of all bonds. The advantage of this notation is that only the position of one monomer has to be stored plus the orientations of all bonds. The polymer in Fig. 2, for example, is described by the position of the first monomer, on the left side of the figure, and **+x−y+z+x−x+z**.

The dynamics can be described in terms of bonds. The bonds that are located on both ends of the polymer are always free to change. The internal bonds are free to change only when they are part of a pair of oppositely oriented neighboring bonds (a kink). The first and last bond in Fig. 2 can change to any new bond: **+x**, **+y**, **+z**, **−x**, **−y** or **−z**. The kink configuration **+x−x** can change into any new kink: **+x−x**, **+y−y**, **+z−z**, **−x+x**, **−y+y**, or **−z+z**.

A. Multispin coding

With multispin coding, many polymers can be simulated in parallel. We used an approach similar to the one by Barkema and Krenzlin.[12] The idea is to write the most time consuming parts of the simulation using only the logical instructions *and* ($\wedge$), *or* ($\vee$), *exclusive or* ($\oplus$), and *not* ($\neg$); since those instructions work on the individual bits of an integer, each logical operation can be done for many polymers at once. Our implementation used 64-bit unsigned integers to simulate 64 different polymers in parallel. As described in Sec. III, there are six directions a bond can point to, so each bond must be encoded using at least three bits. It is now possible to encode 64 bonds in three integers x, y, and z, as shown in Table I.

In each iteration of the inner loop of the algorithm, a random monomer i, $0 \leqslant i < L$, is selected. When an inner monomer is selected the two surrounding bonds are compared; if they are opposites, they are replaced by a randomly generated pair of opposite bonds. Section III C describes how to generate those bonds. The first and last monomers are handled separately, which is described in Sec. III B.

To find the kinks in all of the 64 polymers, we use the assignment from Eq. (4):

$$k_i = (x_{i-1} \oplus x_i) \wedge (y_{i-1} \oplus y_i) \wedge (z_{i-1} \oplus z_i). \tag{4}$$

Monomer i is surrounded by bonds $i-1$ and i. Bit j of k_i is 1 if the surrounding bonds of monomer i of polymer j are in opposite directions.

If a monomer can be moved, it will be relocated using a list of random kinks encoded in $\hat{x}$, $\hat{y}$, and $\hat{z}$. Bonds $i-1$ and i that surround monomer i are replaced by $\hat{x}$, $\hat{y}$, and $\hat{z}$ and their binary complements, respectively. Equation (5) shows how this can be done:

$$\begin{aligned} x_{i-1} &= (\neg k_i \wedge x_{i-1}) \vee (k_i \wedge \hat{x}), \\ x_i &= (\neg k_i \wedge x_i) \vee (k_i \wedge \neg \hat{x}), \end{aligned} \tag{5}$$

and similar statements for y and z. With only 27 logical operations the kinks near monomer i in all 64 polymers are replaced by new kinks, while polymers that have no kink near monomer i are left unaltered.

B. First and last monomer

The first and last monomers are always free to move. When one of those monomers is selected we can just replace the bonds with randomly generated bonds: $x_0 = \neg \hat{x}$, $y_0 = \neg \hat{y}$, $z_0 = \neg \hat{z}$ if monomer 0 was selected and $x_{L-2} = \hat{x}$, $y_{L-2} = \hat{y}$, and $z_{L-2} = \hat{z}$ if monomer $L-1$ was selected. Equation (5), with $k_i = 1$, tells us that we have to use the binary complement of the random kink when monomer 0 is moved.

The complicating factor is that we need to keep track of the position of the first monomer. We have to calculate the distances traveled in the x, y, and z directions. Since those directions are equivalent, we only calculate $r = x + y + z$. For this we only need to know whether the first bonds point at a negative direction, which is one of **−x**, **−y**, and **−z**. This is done using the following equation:

$$d = (x_0 \wedge y_0) \vee (y_0 \wedge z_0) \vee (z_0 \wedge x_0). \tag{6}$$

We do this both before and after we insert the random bonds. With this information we can calculate the new positions of the first monomers:

$$r_i = r_i - 2d^{(i)}_{\text{before}} + 2d^{(i)}_{\text{after}}. \tag{7}$$

This part of the simulation could not be efficiently implemented with multispin coding; we left it as a loop over all 64 polymers.

C. Generation of random kinks

The algorithm described above relies on the availability of random kinks. These kinks should be generated with the probabilities as given in Eq. (2). Since the two bonds in a kink have opposite directions, only one bond has to be generated; the bond on the other side of the monomer is easily derived.

The properties of detailed balance are used to create those bonds correctly. Certain properties must be enforced: first of all the **x**, **y**, and **z** directions should occur with the same probability; secondly the ratio of the probabilities for $+$ and $-$ bonds is given by quotient of P^- and P^+, as given in Eq. (2); this quotient is given by

$$P^{\mathrm{rel}} = P^- / P^+ = e^{-2E}. \tag{8}$$

The first property is enforced by rotating some of the bonds (we used 50%) the following way: **x**↦**y**, **y**↦**z**, and **z**↦**x**. Using a randomly generated bit pattern r the following statements are used to rotate the bonds:

$$\begin{aligned} \tilde{x} &= (r \wedge \hat{x}) \vee (\neg r \wedge \hat{y}), \\ \tilde{y} &= (r \wedge \hat{y}) \vee (\neg r \wedge \hat{z}), \\ \tilde{z} &= (r \wedge \hat{z}) \vee (\neg r \wedge \hat{x}). \end{aligned} \tag{9}$$

The second property is then enforced by inverting some of the bonds. With 50% probability, the negative bonds are inverted and with P^{rel} times 50% the positive bonds are inverted. To make sure that all random kinks are independent we create a list of those and reshuffle this list regularly.

IV. RESULTS

The simulation algorithm described in Sec. III was implemented using the C programming language. We used a lagged (24, 55) additive Fibonacci random number generator. The simulations are done on a Silicon Graphics Origin 200 (180 Mhz) and on a DEC Alpha (466 Mhz) computer. The latter is faster and takes about 1.1 μs for 64 simultaneous Monte Carlo steps for $L=100$. We have performed simulations for lengths up to 200. The CPU time taken to calculate the drift velocity varied from a few seconds for small polymers up to about 17 hours for the longest polymers ($L=200$) in the smallest electric field ($E=0.001$).

The polymers where initialized in a U-shape with both ends in the direction of the electric field. At regular intervals we checked whether the center-of-mass of a polymer has moved at least its own size, which is the maximum distance between any two monomers. When this has occurred for a polymer, we assume that the polymer has thermalized; the measurement starts after this thermalization. The measurement is stopped when all polymers have thermalized and the average distance traveled by all polymers is a few times their own size. We assume that measurements are statistically independent when a polymer has traveled a distance equal to its own size.

A. Drift velocity

The results of our simulations are presented in Fig. 3. The short polymers, up to length 20, show no superlinear dependence on the velocity on the electric field. When a small force, $E \ll L^{-1}$, is applied to the polymers, the velocity of the polymers varies linearly with the electric field. When a force around $E \approx L^{-1}$ is applied to the longer polymers, the polymer velocity depends superlinearly on the electric field. We show in Sec. IV C that the dependence becomes quadratic for long polymer chains, as derived in Sec. II B. For much larger electric fields, the velocity decreases to zero. For $E \sim 1$, it is known that the Monte Carlo approach is not realistic.[13] From Fig. 3, we see that the decrease sets in for much lower electric field strengths ($E_h \ll 1$). This is evidence that this velocity decrease is a real effect, not an artifact of this model.

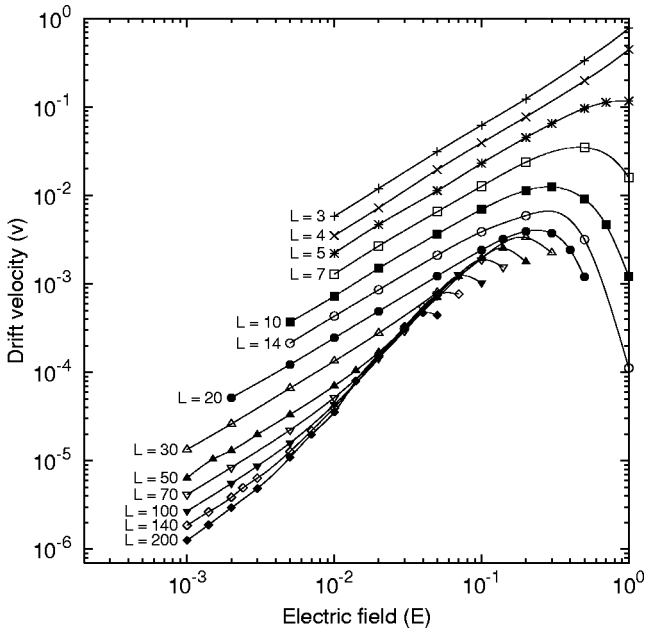

FIG. 3. Drift velocity v of polymers of lengths L up to $L=200$ in electric fields between $E=0.001$ and $E=1$.

For polymer length $L=100$ we performed some short simulations to get insight in the typical movement of the center-of-mass of the polymer. In Fig. 4 the position of the center-of-mass, scaled with a factor of E^{-1}, is plotted as a function of time, for different field strengths. The starting positions of the polymers are chosen such that the graphs do not overlap. For the smallest electric fields the movement is just like one would expect from a diffusing particle, it moves randomly, but with some preferred direction. For the electric field in the middle range, the diffusion effect becomes relatively smaller. This results in a smoother behavior. In high electric fields the movement of the center-of-mass sometimes halts, when the force on the ends of the polymer pulls the polymer into a U-shape. When this happens the polymer has to untangle itself before its center-of-mass can move forward again.

B. Polymer shapes

The polymer shape in a small electric field resembles a random walk, as shown on the left side of Fig. 5. When the electric field is increased, the shape becomes stretched parallel to the electric field;[14] the configuration may be viewed as a set of blobs which move independently, as discussed in Sec. II B. As shorter polymers move more quickly in a given electric field, the blob configuration moves faster than a random walk configuration which results in a superlinear increase of speed when the electric field is changed. When the electric field is increased above a certain value the shape may transform into a U-shape, as shown in Fig. 6. With higher

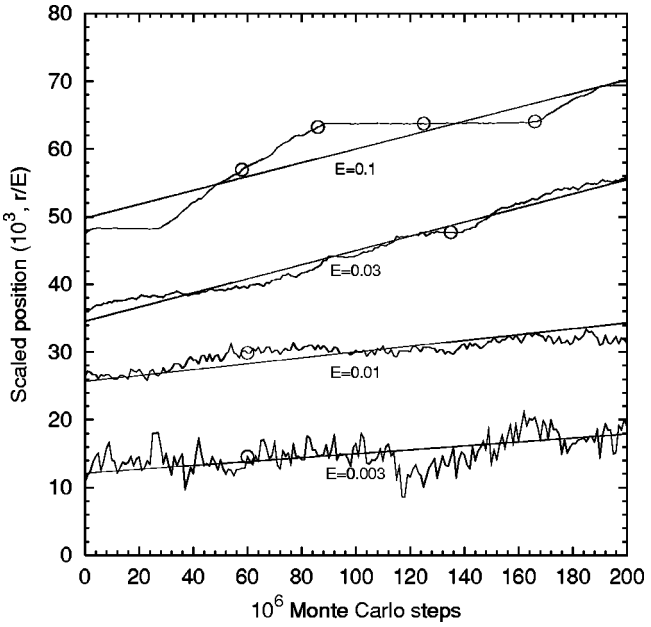

FIG. 4. The position of the center-of-mass of a polymer as a function of the number of Monte Carlo steps. The sample polymer has length $L=100$ and the position is divided by the applied electric field. The straight lines indicate the average velocity. From top to bottom, the electric field is $E=0.1$, 0.03, 0.01, and 0.003. The circles denote the locations where snapshots are taken of the polymer configuration; these are shown in Figs. 5 and 6.

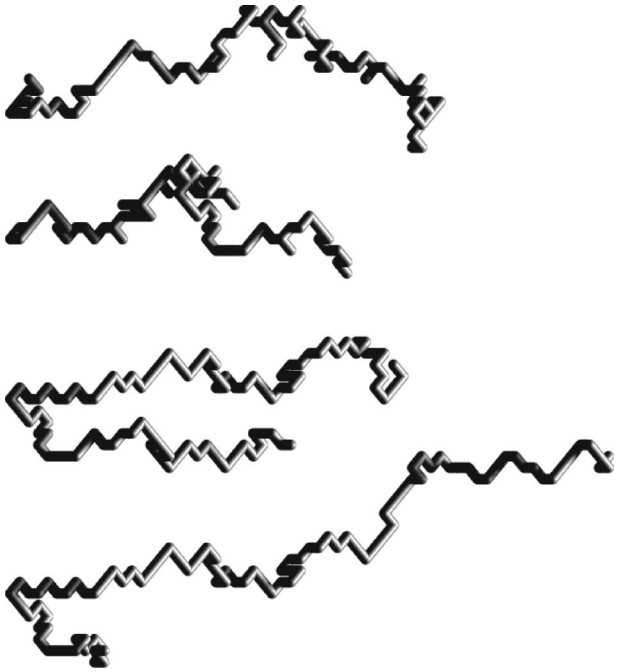

FIG. 6. Snapshots of a polymer of length 100 in an applied electric field $E=0.1$. In high electric fields the polymer does not look like a random walk, and the dynamics become complex. The center-of-mass displacement is shown in Fig. 4. From top to bottom the snapshots are taken at Monte Carlo steps: 5.8×10^7, 8.6×10^7, 1.25×10^8, and 1.66×10^8.

electric fields it becomes more difficult to escape from this U-shape. Since the polymer cannot move sideways it is trapped in the lattice for a long time compared to the time it moves.

Figure 6 shows polymers in different configurations. The first polymer is stretched in the direction of the electric field. This configuration may be viewed as a large number of very small blobs. As such, the polymer has a high velocity, which may also be seen in Fig. 4 near 5.8×10^7 Monte Carlo steps. The second polymer is a transition configuration between the fast-moving cigar-like configuration as described above, and the U-shape configuration. The polymer forms a hernia,[13,15] which decreases the speed of the polymer locally. When the trailing end of the polymer passes the hernia, the third configuration appears. This polymer has a typical U-shape: the two ends both point into the direction of the electric field and much of the stored length diffuses out of the polymer. The motion of the center-of-mass stops, as can be seen in Fig. 4 near 1.25×10^7 Monte Carlo steps. The only way to escape from the U-shape is to create stored length at the shorter end of the polymer, and then transport it all the way against the electric field to the back of the polymer. It takes an exponential time to escape from the U-shape.[13] Just before the polymer escapes from the U-shape, like the fourth polymer, its configuration is stretched and has almost no stored length. This state transforms quickly into a state that resembles the state of the first polymer in Fig. 6.

FIG. 5. Three polymers of length $L=100$ in different electric fields. From left to right: $E=0.003$, 0.01, and 0.03. Polymers in small electric fields look like random walks; in slightly larger electric fields the ends tend to protrude. The center-of-mass displacement of these three polymers is shown in Fig. 4.

For small electric fields the polymer configuration is known to resemble a three dimensional random walk. The average number of kinks is thus expected to be 1/6. For higher electric fields the U-shape configuration becomes more frequent. In this configuration the kinks are likely to diffuse towards the ends of the polymer, which means that the average number of kinks in the middle of the polymer decreases. When this happens we can no longer apply the blob argument as described in Sec. II B. The mobility of the blobs in the middle of the polymer decreases as the average number of kinks in that region decreases. To check the dependence of stored length on the electric field we have performed some short simulations to find the average number of kinks on each location along the polymer. The simulations consisted of 10^9 Monte Carlo steps after 2×10^8 steps of thermalization, starting with a random configuration. Every 10^6 Monte Carlo steps the kinks are counted. The fraction of time that a kink exists on a certain location is displayed in Fig. 7. Duke[16] showed that the chain of monomers in the repton model loses stored length, when subjected to electric fields. Here we find that the cage model shows a similar property. The amount of stored length is, on average, decreasing in the middle of the polymer when increasing the field strength.

For high electric fields, $E>L^{-1}$, the dynamics of the polymer becomes unstable: hernias are created along the polymer, which effectively reduce the number of kinks trans-

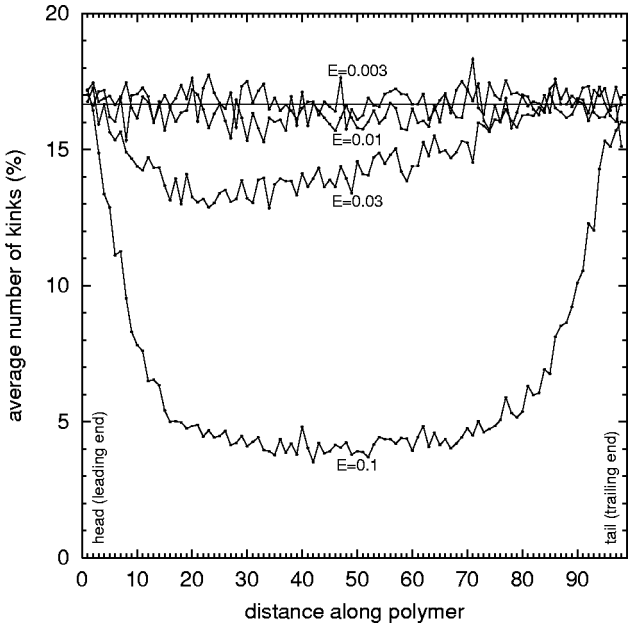

FIG. 7. The average number of kinks as a function of the distance along the polymer; the end monomer that has the lower potential energy is the head of the polymer. The polymers are of length 100 and the electric fields are $E=0.003$, 0.01, 0.03, and 0.1. The line gives the expected value 1/6 of kinks in a random walk.

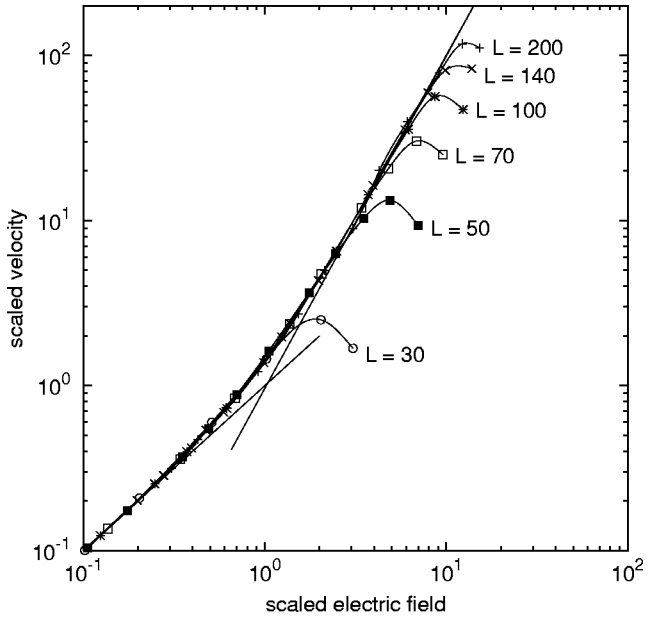

FIG. 8. Transition between the linear and quadratic dependence of the velocity on the electric field. For various polymer lengths, the scaled velocity $v'=(\sqrt{b}/a)v$ is plotted as a function of scaled electric field $E'=(\sqrt{b/a})E$, where a and b are L-dependent parameters given in Table II. The curve is given by $v'=\sqrt{E'^2+E'^4}$; the straight lines indicate linear and quadratic behavior.

ported to the leading end of the polymer. This results in a lower mobility of the leading part of the polymer, while the mobility of the trailing end is not affected. The polymers are likely to form the U-shaped configurations. In this configuration, both ends of the polymer point forward which results in a decrease of kinks near the base of the U-shape. Both effects are shown in Fig. 7 for polymers of length 100. For $E=0.03$, the uneven distribution of kinks is clearly visible and for $E=0.1$, the number of kinks in the middle of the polymer is clearly much lower than 1/6. When the density of kinks becomes less than 1/6 per monomer, the elastic force that contracts the polymer is no longer in balance with the electric force. The polymer itself now transports the force along the chain, which may be better explained by the continuous model of Deutsch and Madden.[13]

C. Comparisons to previous reports

The results of the Duke–Rubinstein model have been compared to actual experiments.[17] For longer polymers, the data is well described by

$$\frac{L^2 v}{\alpha}=\left[\left(\frac{LE}{\beta}\right)^2+\left(\frac{LE}{\beta}\right)^4\right]^{1/2}. \tag{10}$$

This function is equivalent to the function $v^2=aE^2+bE^4$, where a and b are functions of α, β, and L. To check whether our results show the same scaling behavior, we collapsed our data to the function $v'=\sqrt{E'^2+E'^4}$, in Fig. 8, where $v'=(\sqrt{b}/a)v$ and $E'=(\sqrt{b/a})E$. The data in the third regime is discarded for the calculation of a and b (see Table II).

Experiments have been performed on electrophoresis;[18,19] both articles confirm the existence of regions where $v\sim E$ and $v\sim E^2$. To the best of our knowledge, the third regime has not been observed directly. The cycle of configurational changes for $L=100$, $E=0.1$, as described in Sec. IV B, occurs on the boundary between the second and third regime, where the times spent in the cigar-like configuration, typical of the second regime, and the U-shape configuration, typical of the third regime, are similar. Rampino,[20] and Howard and Holzwarth[21] separately observe a similar cycle of conformational changes for electrophoresis of DNA stands in a gel.

The diffusion constant is $D=\sqrt{a}/L$. The scaling found by Barkema and Krenzlin[12] is given by $DN^2=0.173+1.9N^{-2/3}$, where $N=L-1$. Figure 9 shows our results compared to their scaling function. Our results agree within statistical errors.

V. CONCLUSIONS

The cage model is extended to simulate gel electrophoresis, and the drift velocity of polymers in a gel is measured as

TABLE II. Values for L^2a and b, obtained by fitting the drift velocity to the form $v^2=aE^2+bE^4$; these values are used for scaling in Fig. 8. The numbers in parentheses show the statistical error (68% confidence) in the last digit. The graphs of L^2a and b show evidence of convergence to a constant; this is in agreement with Eq. (10).

L	L^2a	b
30	0.166(6)	0.020(2)
50	0.112(4)	0.055(2)
70	0.088(2)	0.084(2)
100	0.0732(7)	0.112(1)
140	0.0649(8)	0.130(1)
200	0.059(5)	0.141(7)

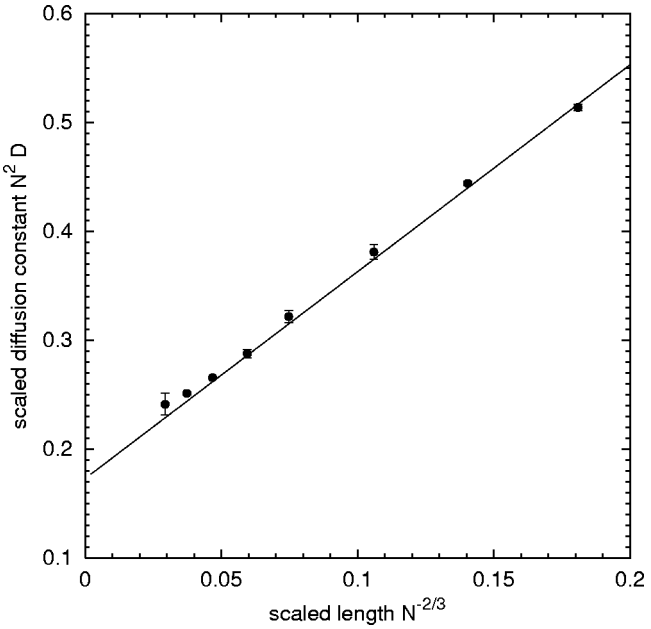

FIG. 9. Diffusion constant calculated from our measurements, compared to the scaling relation found by Barkema and Krenzlin. This scaling relation is a straight line when N^2D is plotted as a function of $N^{-2/3}$.

a function of polymer length L and electric field strength E. The polymers behave differently in three regimes of the electric field: in a small electric field ($EL \ll 1$) the velocity depends linearly on the electric field, in a high electric field ($E > E_h$) the polymers are likely to be trapped in a U-shape, probably caused by buildups of stored length protruding from the confining tube of the polymer, so-called hernias. The regime in between shows a superlinear dependency on the electric field, as reported earlier for the Duke–Rubinstein model. The Duke–Rubinstein model does not allow the formation of hernias, which probably causes the difference in behavior for high electric fields.

The typical configuration of a polymer in absence of an electric field is a random walk. When a small electric field is switched on, the polymer stretches in the direction of the electric field. When the electric field is increased above a certain threshold, this typical polymer configuration becomes unstable: hernias form along the polymer chain, which decrease the mobility locally. The result is that the trailing end of the polymer folds forward, producing a U-shaped configuration from which the polymer must escape before it can move forward again.

The average number of kinks is not uniformly distributed over the polymer in electric fields $E > L^{-1}$. The two main contributions come from the cigar-like configuration and the U-shaped configuration. If the polymer has a cigar-like shape, kinks appear at the trailing end of the polymer and disappear at the front end. When a hernia forms somewhere in the middle of the chain it tends to grow: kinks move into the hernia more frequently than they move out of the hernia. The result is that the trailing end of the polymer has more stored length, and therefore a higher mobility, than the forward pointing part of the polymer. The U-shaped configuration also contributes to an uneven distribution of the kinks along the chain: since both ends of the polymer point forwards, the kinks diffuse out of the polymer.

ACKNOWLEDGMENTS

We thank G. T. Barkema and A. G. M. van Hees for useful discussion. The High-Performance Computing Group of Utrecht University is gratefully acknowledged for ample computer time.

[1] P. G. de Gennes, J. Chem. Phys. **55**, 572 (1971).
[2] T. T. Perkins, D. E. Smith, and S. Chu, Science **264**, 819 (1994).
[3] M. Rubinstein, Phys. Rev. Lett. **59**, 1946 (1987).
[4] K. E. Evans and S. F. Edwards, J. Chem. Soc., Faraday Trans. 2 **77**, 1891 (1981).
[5] M. Prähofer and H. Spohn, Physica A **233**, 191 (1996).
[6] M. E. J. Newman and G. T. Barkema, Phys. Rev. E **56**, 3468 (1997); G. T. Barkema and M. E. J. Newman, Physica A **244**, 25 (1997).
[7] T. A. J. Duke, Phys. Rev. Lett. **62**, 2877 (1989).
[8] G. T. Barkema, J. F. Marko, and B. Widom, Phys. Rev. E **49**, 5303 (1994).
[9] A. van Heukelum, G. T. Barkema, and R. H. Bisseling (unpublished).
[10] J. M. Deutsch and T. L. Madden, J. Chem. Phys. **91**, 3252 (1989).
[11] A. Baumgärtner, U. Ebert, and L. Schäfer, J. Stat. Phys. **90**, 1375 (1998).
[12] G. T. Barkema and H. M. Krenzlin, J. Chem. Phys. **109**, 6486 (1998).
[13] J. M. Deutsch and T. L. Madden, J. Chem. Phys. **90**, 2476 (1989).
[14] M. Widom and I. Al-Lehyani, Physica A **244**, 510 (1997).
[15] T. A. J. Duke and J. L. Viovy, Phys. Rev. Lett. **68**, 542 (1992).
[16] T. A. J. Duke, J. Chem. Phys. **93**, 9049 (1990).
[17] G. T. Barkema, C. Caron, and J. F. Marko, Biopolymers **38**, 665 (1996).
[18] C. Heller, T. A. J. Duke, and J. L. Viovy, Biopolymers **34**, 249 (1994).
[19] H. Hervet and C. P. Bean, Biopolymers **26**, 727 (1987).
[20] N. J. Rampino, Biopolymers **31**, 1009 (1991).
[21] T. D. Howard and G. Holzwarth, Biophys. J. **63**, 1487 (1992).